Ribosome maturation factor Nop53 controls association of the RNA exosome with pre-60S particles

Cepeda et al.

Supporting information

Figure S1. Rrp6 coimmunoprecipitates GFP-Nop53
Figure S2. Different proteins were co-purified with Rrp6 upon Nop53 depletion
Figure S3. Interaction network of the proteins copurified with Rrp6 or Rrp43 upon depletion of Nop53
Figure S4. Nop53 does not affect the exosome assembly/stability
Figure S5. Separation of markers through glycerol gradient centrifugation
Figure S6. Exosome sediments with large complexes in the absence of Nop53
Figure S7. Rrp6-TAP copurifies early pre-rRNAs
Figure S8. Depletion of Nop53 does not affect Rrp6 subcellular localization

Table S1. List of the proteins grouped in a Venn diagram (Fig. 2A)
Table S2. List of the proteins shown in a volcano plot (Fig. 2B)
Table S3. List of the proteins grouped in a Venn diagram (Fig. 4)

Experimental Procedure

Fluorescence microscopy

Cells were fixed in 70% methanol for 15 minutes, rinsed with cold phosphate-buffered saline (PBS). Cells were observed using a Nikon Eclipse Ti microscope equipped with filters for green fluorescence (GFP-3035B-000-ZERO, Semrock) and red fluorescence (Texas Red BrightLine set; TXRED4040-B, Semrock). The exposure times varied from 1 to 3 seconds. Images were processed and analyzed using the programs Nis Elements (version 3.07; Nikon) and ImageJ (http://rsbweb.nih.gov/ij/).

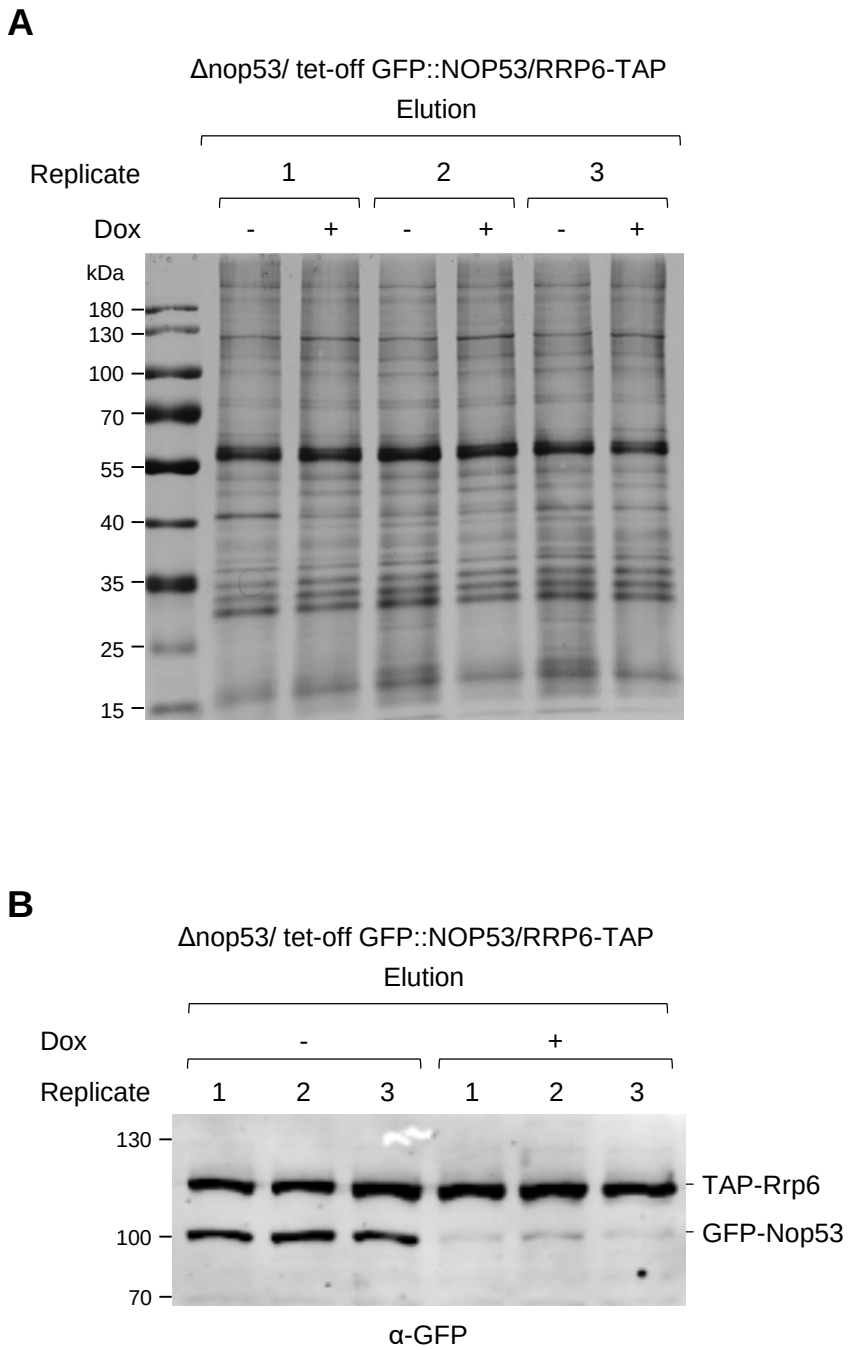

Supp. Figure S1. Rrp6 coimmunoprecipitates GFP-Nop53. To evaluate the effect of Nop53 on the Rrp6 interactome, coimmunoprecipitation assays were performed using the conditional strain *Δnop53/tetOff::GFP-NOP53* carrying the endogenous Rrp6-TAP fusion grown both in the presence (- doxycycline) and absence (+ doxycycline) of Nop53. Both conditions were analyzed in biological triplicates. An aliquot of each elution was resolved by SDS-PAGE and both analyzed by silver staining (**A**) and by western blotting against GFP (**B**), showing that GFP-Nop53 was co-purified with Rrp6, and that the treatment with doxycycline was sufficient to deplete GFP-Nop53.

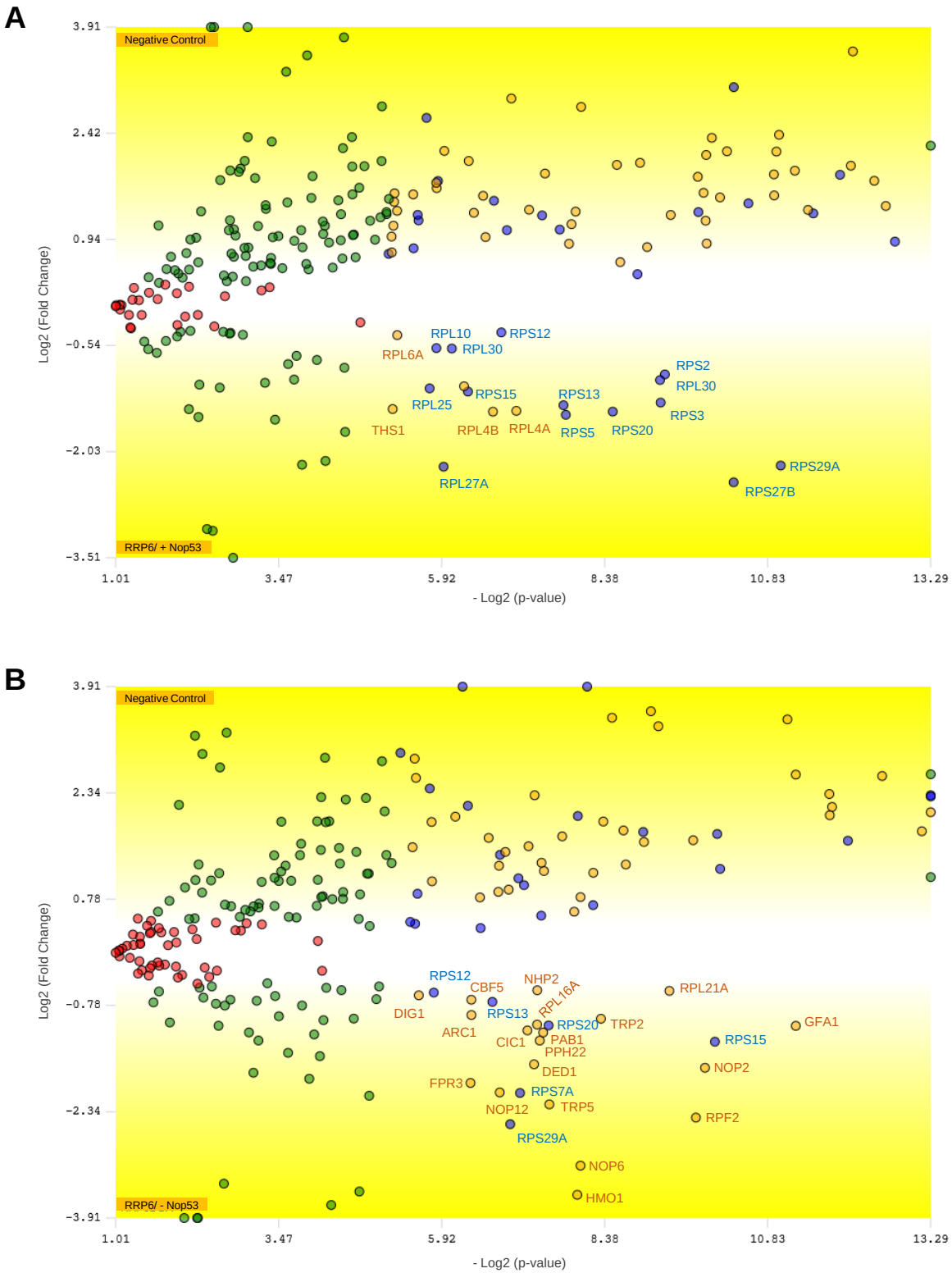

Supp. Figure S2. Different proteins were co-purified with Rrp6 upon Nop53 depletion. As shown in Fig. 3A, 21 and 30 proteins were detected both in the negative control and respectively copurified with Rrp6 in the presence and absence of Nop53. Moreover, 199 proteins were detected in all the three groups. To evaluate which of these proteins (in at least two replicates per group) were significantly enriched with Rrp6 in the presence and absence of Nop53, two independent TFold analyses (BH q-value 0.05; F-Stringency 0.030; L-Stringency 0.400) were performed. The quantitative comparison of proteins copurified with Rrp6 (bottom) and the negative control (top), in the presence (**A**) and upon depletion (**B**) of Nop53, shows in red proteins that did not show a statistically significant change, in green, those that met the fold change criteria, but were not statistically significant, in orange, those proteins of low abundance that met both the fold change and statistical criteria, and in blue, those that met both the fold change and statistical criteria. Listed in blue and orange are only the proteins copurified with Rrp6 significantly enriched relative to the negative control.

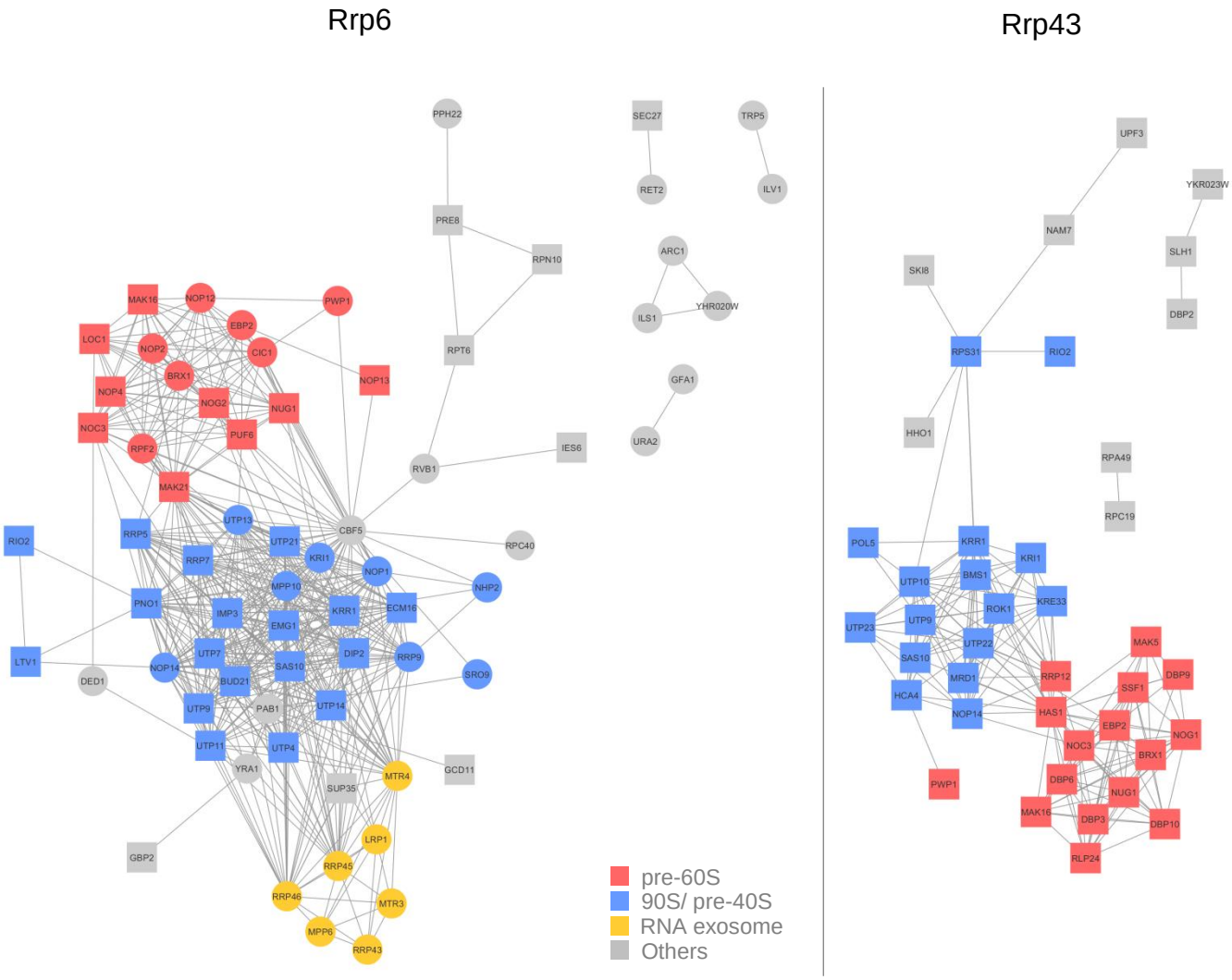

Supp. Fig. S3. Interaction network analysis of the proteins copurified at increased levels with Rrp6 or Rrp43 upon depletion of Nop53. (**A**) Two independent protein interaction networks were created using the STRING database 11.0 (37) with the lists of proteins identified in at least two replicates coimmunoprecipitated with Rrp6 and Rrp43, whose levels were increased upon depletion of Nop53. Coimmunoprecipitated proteins whose levels were significantly increased are depicted as circles, while proteins exclusively identified upon depletion of Nop53 are depicted as squares. The nodes were colored using the software Cytoscape to highlight the most enriched groups: pre-60S (red), 90S/pre-40S (blue), RNA exosome (yellow), others (gray). We have selected the following basic settings for the networks building: Meaning of network edges: Evidence; Active interaction sources: Experiments and Databases; Minimum required interaction score: High confidence (0.700); Max number of proteins to show: query proteins only. The edges connect functionally related nodes based on the evidence (Experiments and Databases) curated by STRING database.

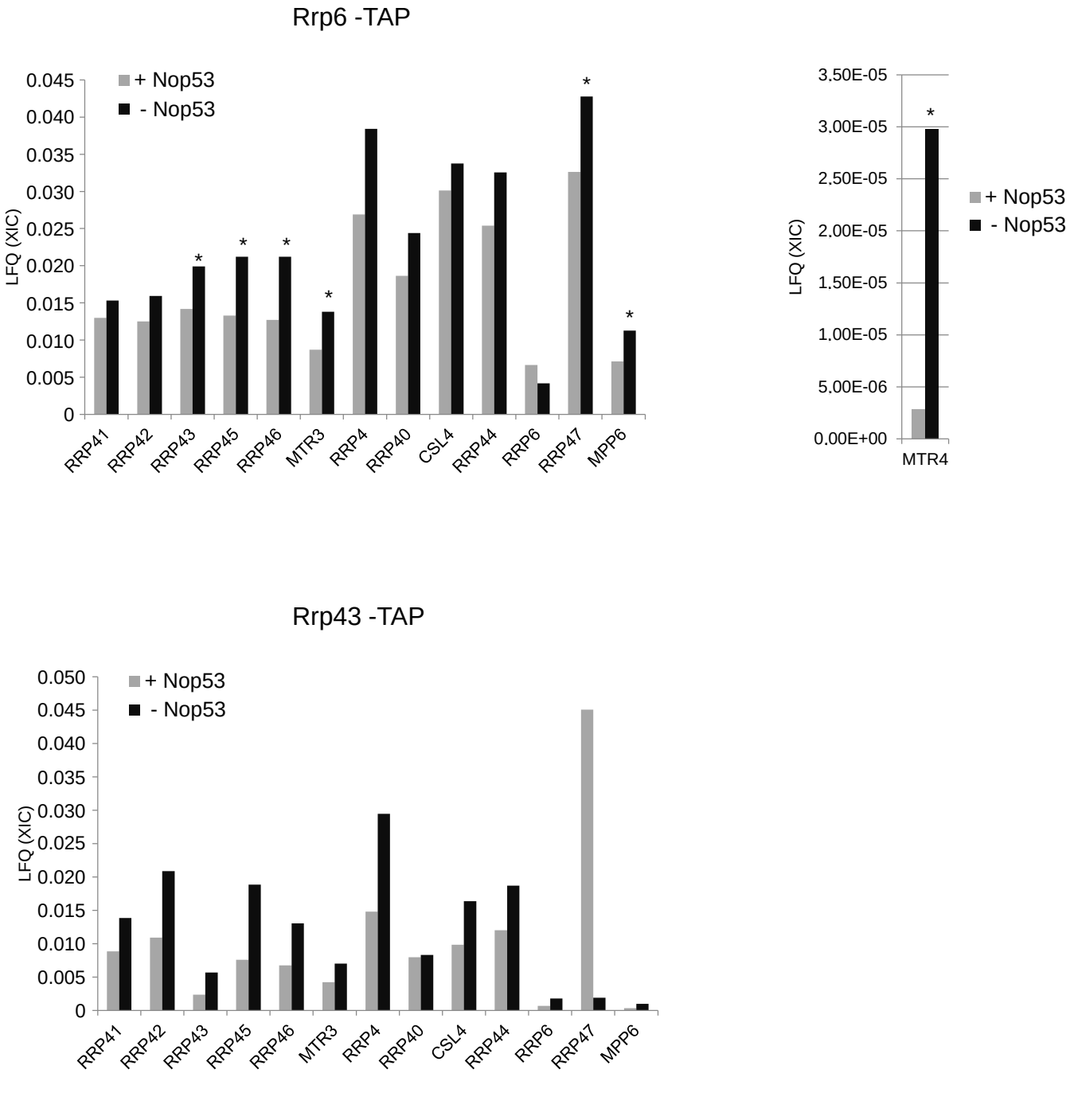

Supp. Figure S4. Nop53 does not affect the exosome assembly/stability. The exosome complex was isolated either with the core subunit Rrp43, or with the nuclear subunit Rrp6, both fused to the TAP tag, in the conditional strain Δ*nop53/tet-Off::GFP-NOP53*. Yeast total extracts obtained from cultures grown in SD medium without or supplemented with doxycycline were subjected to coimmunoprecipitation with IgG sepharose beads. Label free quantitative (LFQ) mass spectrometry analysis based on XIC was carried out. The LFQ values are compared for all exosome subunits and cofactors coimmunoprecipitated with either Rrp6 or Rrp43 in both conditions. All exosome subunits were detected in both conditions in at least 2 replicates both with Rrp43 and Rrp6, indicating that Nop53 depletion does not affect the exosome assembly. (* indicates statistically significant differences (p-value < 0.05))

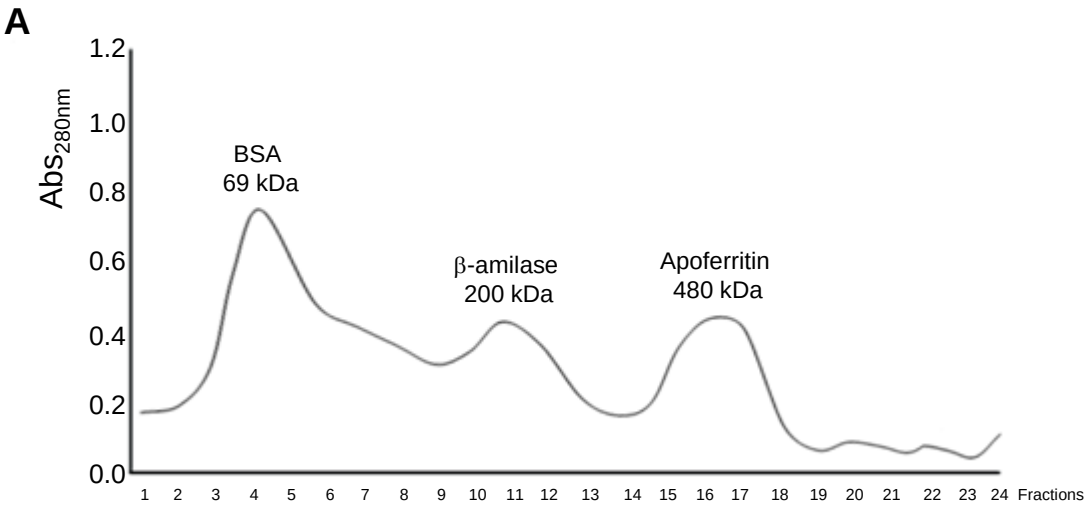

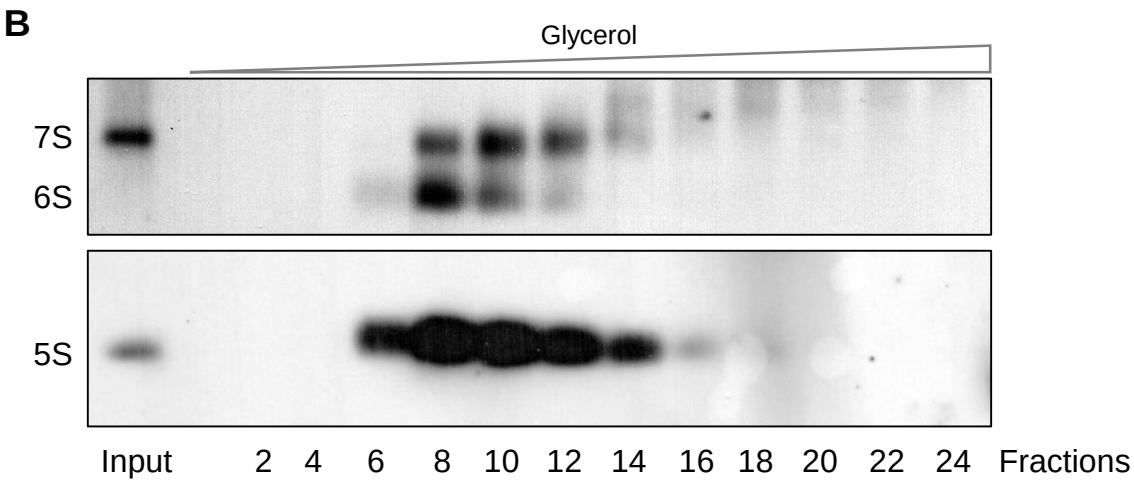

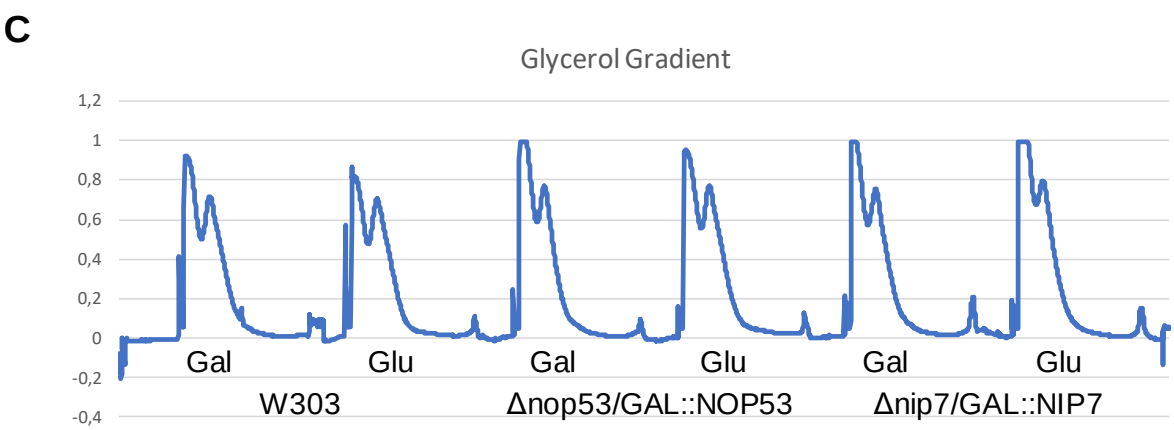

Supp. Figure S5. Separation of markers through glycerol gradient centrifugation. (**A**) Profile of markers separated through glycerol gradient. (**B**) Northern blot of yeast extracts run through similar glycerol gradients to show precursor rRNAs (7S - nuclear and 6S - cytoplasmic), and mature 5S rRNA. (**C**) Examples of separation of total cell extracts through glycerol gradients, which results in similar profiles, independently of the sample.

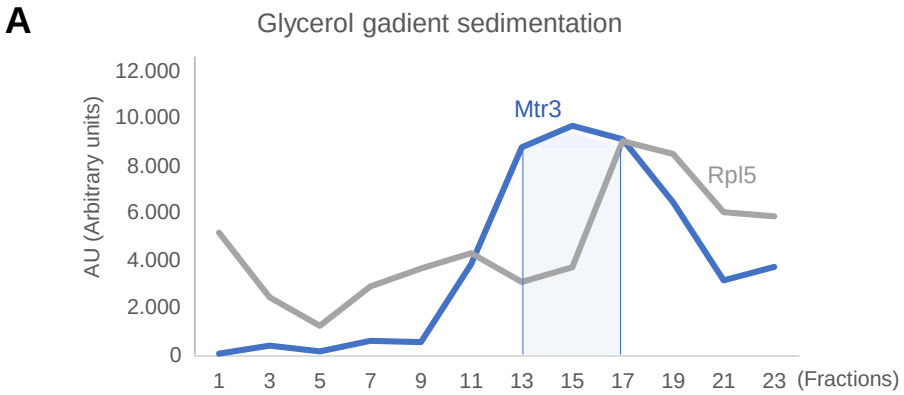

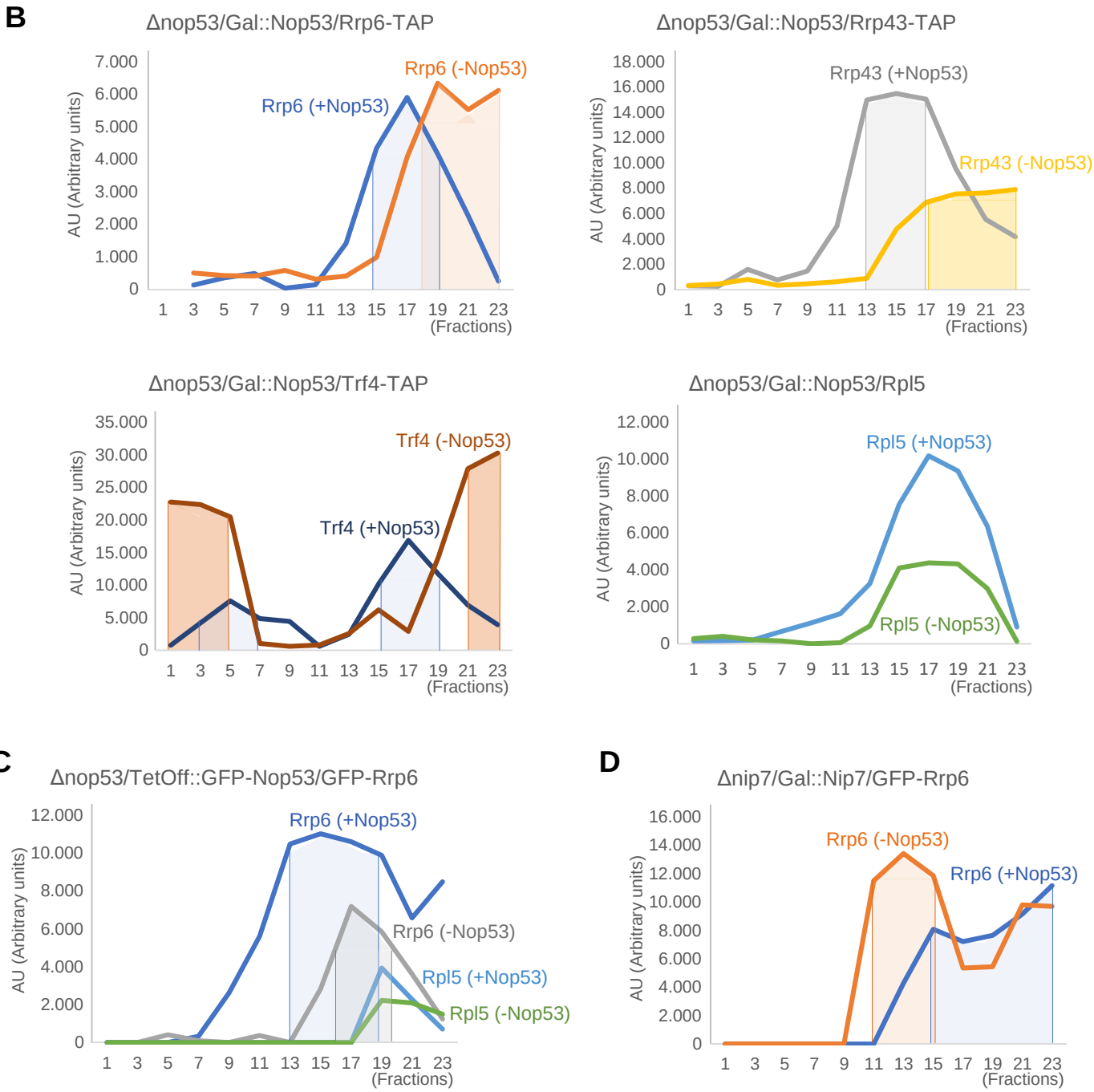

Supp. Figure S6. **Exosome sediments with large complexes in the absence of Nop53.** Quantification of bands from western blots shown in Fig. 7. Bands from the glycerol gradient fractions of the different samples were quantified using Image J. Plots represent the variation of the intensity of each band along the fractions, and show the concentration of the exosome in lower fractions of the gradient in the absence of Nop53. Panels **A**, **B**, **C**, **D** correspond to those of Fig. 7. Colored regions highlight the peaks of concentration of the respective proteins.

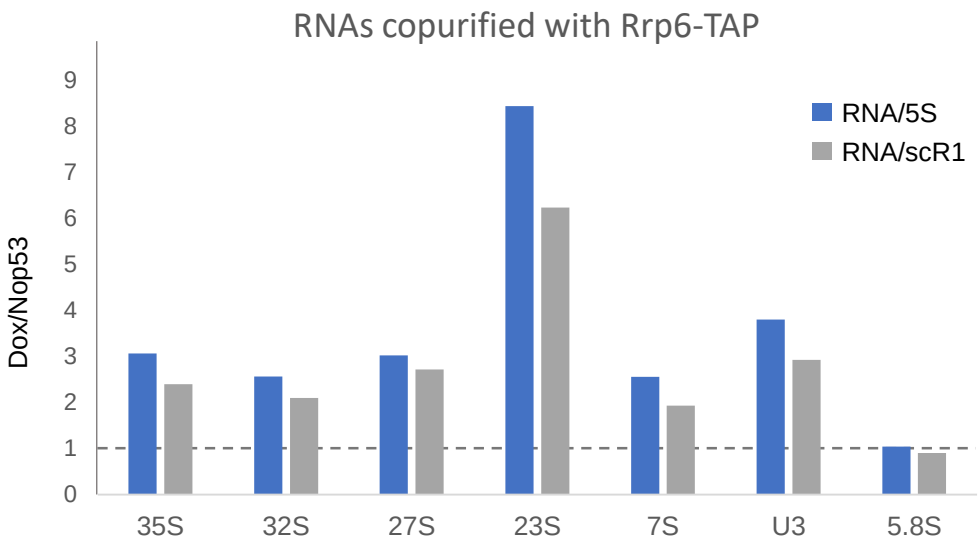

Supp. Figure S7. **Rrp6-TAP copurifies early pre-rRNAs.** Quantification of bands from northern hybridizations shown in Fig. 8. Bands from the elution fractions of both replicates were quantified using Image J and corrected by the levels of co-eluted 5S rRNA or scR1. Graph represents average of ratios of RNAs in the absence of Nop53 relative to its presence (Dox/Nop53), and shows the higher levels of the pre-rRNAs being copurified with Rrp6-TAP upon depletion of Nop53. Because 5S is part of pre-60S particles, its copurification may not only be due its high abundance and might be the reason for the different ratios obtained when comparing 5S and scR1. Note that many pre-rRNAs, such as 35S, could be detected with different probes.

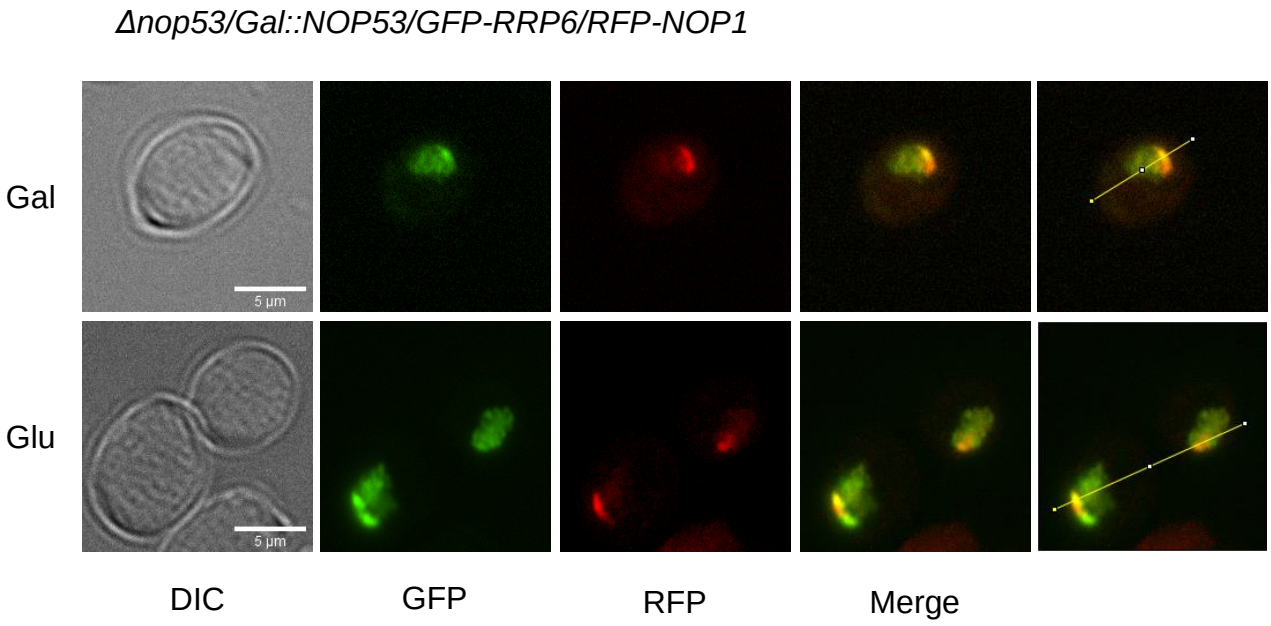

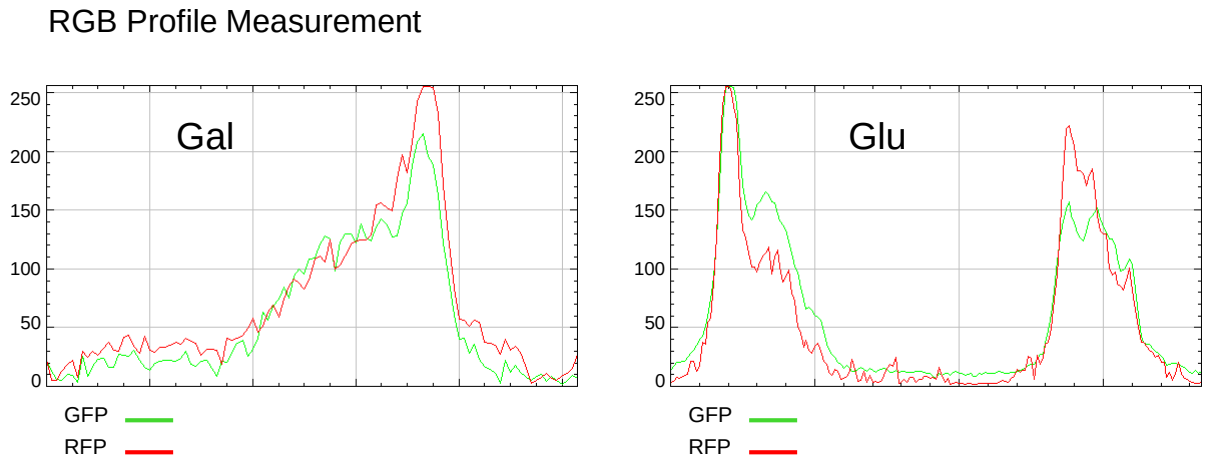

Supp. Figure S8. **Depletion of Nop53 does not affect Rrp6 subcellular localization.** Expression of both GFP-Rrp6 and RFP-Nop1 in Δ*nop53/GAL::NOP53* strain, grown in glucose or galactose and analyzed by fluorescence microscopy (at 100x magnification). The RGB profile was obtained with ImageJ®. Rrp6 shows a nuclear localization, but also co-localizes with Nop1 in the nucleolus.